Land subsidence caused by groundwater exploitation in Suzhou City, China

Chongxi Chen · Shunping Pei · Jiu Jimmy Jiao

Abstract Suzhou City, located at the lower reaches of the Yangtze River in southeastern Jiangsu Province, is one of the few cities in China which suffer from severe ground settlement. A research project was carried out to investigate this problem. Geological and hydrogeological studies show that there is a multi-layered aquifer system with three distinct, soft mud layers of marine and lagoonal origins. An examination of historical records of groundwater extraction, water levels, and ground settlement shows that the ground subsidence is associated with the continuously increasing groundwater extraction in the deep, confined aquifer. It is believed that the consolidation of the soft mud layers, especially the third layer which is thick and close to the main pumped aquifer, contributes to the ground settlement. A three-dimensional finite difference numerical model representing the multi-layered aquifer system was developed to study the ground settlement in response to groundwater extraction. By calibrating the model with both the measured groundwater level and ground settlement, the aquifer parameters were estimated. The model outputs fit reasonably well with the observed results, which indicates that the numerical model can reproduce the dynamic processes of both groundwater flow and soil consolidation. The hydraulic conductivity of the third mud layer near the center of the ground settlement has been reduced by over 30% in the last 14 years. The gradual deterioration in the hydraulic conductivity of the mud may have significant adverse effect on the sustainable groundwater resource of the deep confined aquifer, since the recharge from the shallow aquifers through the mud layer is the only source of water to the deep aquifer. An analysis of the spatial distributions of groundwater drawdown and ground settlement shows that the area with maximum drawdown is not necessarily the area with maximum ground settlement due to the occurrence of the soft mud layer. A simple reallocation in pumping rates on the basis of the spatial distribution of the thick mud layer could significantly reduce the ground settlement.

Résumé La ville de Suzhou, située dans la basse vallée du fleuve Yangtsé dans le sud-est de la province de Jiangsu, est l'une des rares villes de Chine qui souffrent cruellement de tassements du sol. Un projet de recherche a été mené pour étudier ce problème. Des études géologiques et hydrogéologiques montrent qu'il existe un système aquifère multicouche constitué de trois niveaux distincts de limons non consolidés d'origine marine et lagunaire. Un examen des historiques des prélèvements d'eau souterraine, des niveaux de nappe et des tassements de sol montrent que la subsidence du sol est associée à des prélèvements continuellement croissants d'eau souterraine dans l'aquifère captif profond. On pense que le compactage des couches limoneuses non consolidées, en particulier de la troisième couche qui est épaisse et proche du principal aquifère pompé, contribue aux tassements du sol. Un modèle numérique aux différences finies en trois dimensions, représentant l'aquifère multicouche, a été réalisé pour étudier les tassements du sol en réponse aux prélèvements d'eau souterraine. Les paramètres de l'aquifère ont été estimés par calibration du modèle au moyen à la fois des niveaux piézométriques et des tassements du sol. Les résultats de la simulation s'ajustent convenablement aux résultats observés, ce qui indique que le modèle numérique peut reproduire les processus dynamiques aussi bien des écoulements souterrains que de compactage du sol. La conductivité hydraulique de la troisième couche de limon non consolidé au voisinage du centre du tassement de sol a été réduit de plus de 30% au cours des 14 dernières années. La dégradation progressive de la conductivité hydraulique du limon peut avoir un effet significatif néfaste sur la pérennité de la ressource en eau souterraine dans l'aquifère captif profond, puisque la recharge à partir des aquifères superficiels au travers de la couche de limon est la seule alimentation de l'aquifère profond. Une analyse des dis-

Received: 11 March 2002 / Accepted: 5 August 2002
Published online: 25 September 2002

© Springer-Verlag 2002

C. Chen (✉)
Institute of Environmental Geology,
China University of Geosciences, Wuhan 430074, China
e-mail: chongxi@mail.cug.edu.cn

S. Pei
School of Earth and Space Sciences, Peking University,
Beijing 100871, China

J.J. Jiao
Department of Earth Sciences, University of Hong Kong,
Pokfulam Road, Hong Kong, China

 DOI 10.1007/s10040-002-0225-5

tributions spatiales de l'abaissement du niveau piézométrique et des tassements du sol montre que la région soumise à l'abaissement maximal de piézométrie n'est pas nécessairement celle des tassements maximaux du sol liés à la présence de la couche de limon non consolidé. Une simple révision des débits de pompage basée sur la distribution spatiale de la couche de limon épaisse peut réduire significativement les tassements du sol.

Resumen La ciudad de Suzhou, situada en el tramo inferior del Río Yangtze, al sudeste de la provincia de Jiangsu, es una de las pocas ciudades chinas que padece problemas serios de subsidencia. Esto ha motivado la realización de un proyecto de investigación en la zona. Estudios geológicos e hidrogeológicos apuntan a un modelo de acuífero multicapa, con tres niveles distintos de lodos blandos de orígenes marino y lacustre. Examinando los registros históricos de extracciones de agua subterránea, así como de nivel piezométrico y de subsidencia, se observa que ésta se halla asociada al bombeo cada vez mayor del acuífero confinado profundo. La hipótesis es que las capas de lodos blandos se van consolidando, si bien la que más contribuye a ello es la tercera, potente y próxima al acuífero más explotado. Se ha realizado un modelo numérico tridimensional en diferencias finitas que representa el sistema acuífero multicapa, con lo que se puede estudiar el efecto de la extracción de agua subterránea en la subsidencia. Calibrando el modelo con niveles piezométricos medidos y con datos de subsidencia, se ha podido estimar los parámetros del acuífero. Los resultados del modelo ajustan de forma razonable con los datos medidos, por lo que el modelo numérico es capaz de reproducir los procesos dinámicos de flujo de aguas subterráneas y consolidación del terreno. La conductividad hidráulica de la tercera capa de lodo cerca del centro de asentamiento se ha reducido en más del 30% durante los últimos 14 años. El deterioro gradual de la conductividad hidráulica del lodo puede tener efectos adversos notables en la sustentabilidad de los recursos de agua subterránea del acuífero confinado profundo, ya que se recarga exclusivamente de acuíferos más someros a través de la capa de lodo. El análisis de la distribución espacial de descenso del nivel piezométrico y de subsidencia muestra que el área de extracción máxima no coincide necesariamente con la de máxima subsidencia, debido a la existencia de la capa de lodos blandos. Una mera redistribución de los caudales de bombeo en función de las propiedades espaciales de la gruesa capa de lodos podría reducir drásticamente los problemas de subsidencia.

Keywords Groundwater · Land subsidence · Numerical simulation · Finite difference · Nonlinear consolidation

Introduction

Land subsidence due to large amounts of fluid withdrawal from an aquifer or hydrocarbon reservoir has occurred in numerous regions throughout the world and has been extensively investigated both quantitatively and qualitatively by previous researchers (Pratt and Johnson 1926; Poland and Davis 1969; Lewis and Schrefler 1978). Such subsidence is attributed to the consolidation of sedimentary deposits as the result of increasing effective stress (Bell et al. 1986). Pratt and Johnson (1926) showed that land subsidence resulted directly from lowering of the piezometric surface due to fluid extraction. Poland and Davis (1969) demonstrated that the centers of subsidence in the Santa Clara valley, California, USA coincided with the centers of major pumping, and the historical development of the subsidence coincides with the increased utilization of groundwater. Abidin et al. (2001) show that land subsidence in Jakarta in Indonesia is strongly related to excessive groundwater extraction.

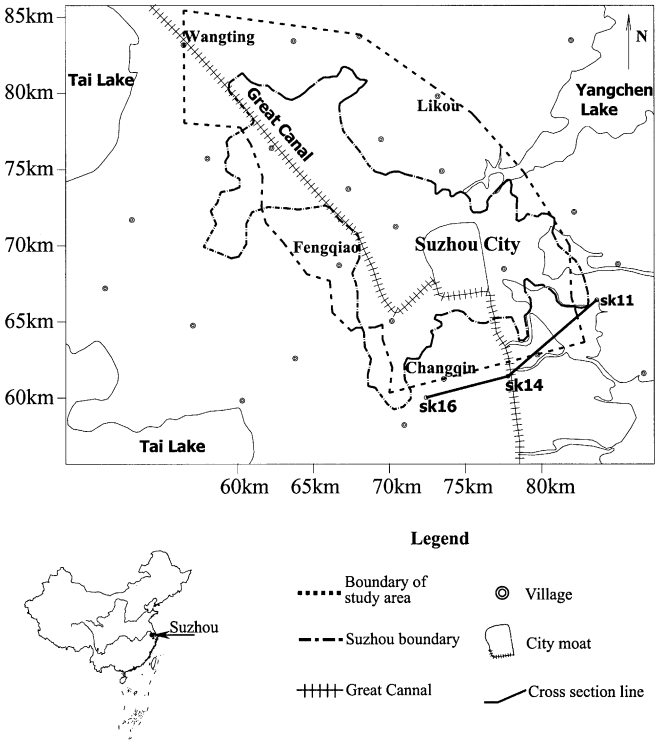

Fig. 1 Location of Suzhou City and the study area in China

There are a few cities in China, including Suzhou City, which have reported increasingly severe ground subsidence caused by extensive groundwater exploitation. Located at the lower reaches of the Yangtze River in the southeastern Jiangsu Province (Fig. 1), Suzhou City has been a famous historical and cultural center and an important hub of communications in the coastal areas of China. It has a population of almost 6 million. The severe ground settlement, with maximum accumulative land subsidence in some locations exceeding 1 m in 1980–1997, has caused social and economic problems.

This research project has been carried out to study the characteristics, patterns and mechanisms of ground subsidence in Suzhou City. The geology and hydrogeology of the city area were studied to set up a hydrogeological conceptual model. Borehole data were analyzed to ob-

 DOI 10.1007/s10040-002-0225-5

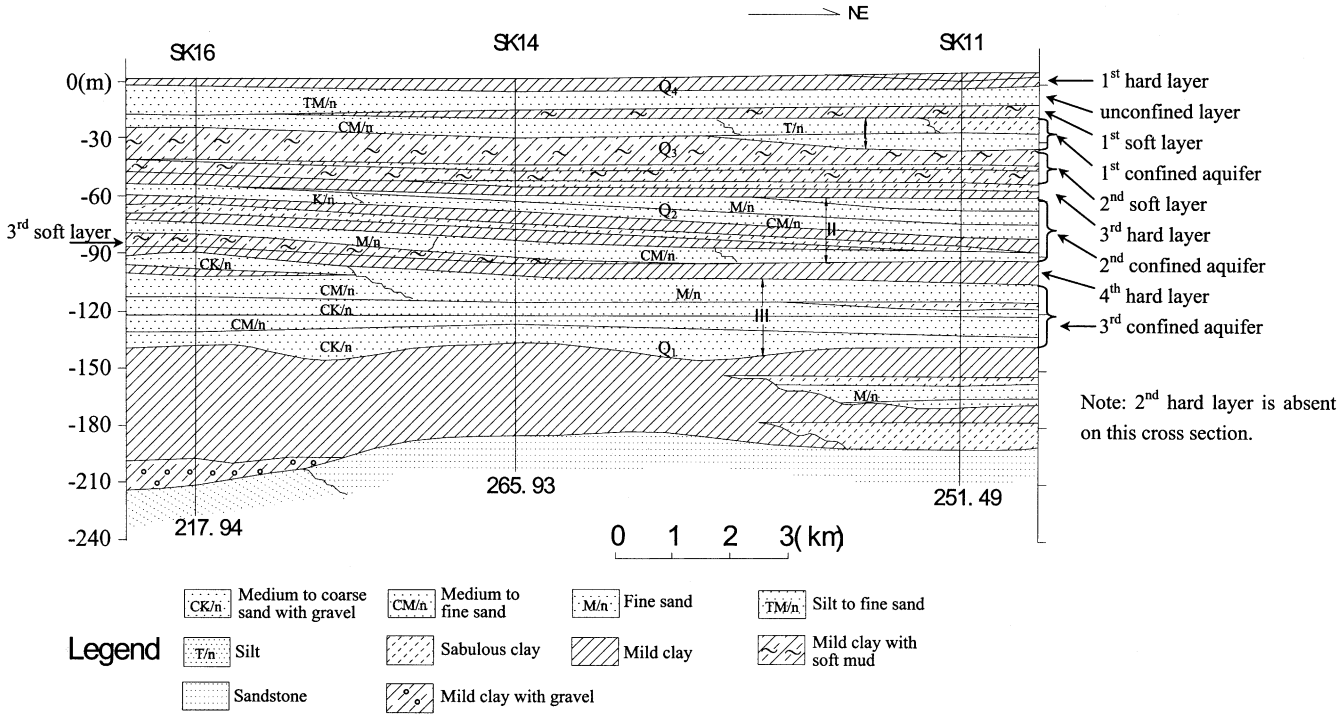

Fig. 2 Hydrostratigraphy along the cross-section line *Sk16–Sk14–Sk11*

tain the spatial distribution of the aquifers and aquitards. Water-level dynamics and temporal variations of groundwater withdrawal were examined to understand the impact of utilization of groundwater on the hydrogeological system.

A three-dimensional numerical model which couples the flow and consolidation was developed to simulate water level and ground settlement. Aquifer parameters were estimated by calibrating the model against the observed water level and settlement data. The simulated and the observed groundwater levels and ground settlement were carefully compared to examine the performance of the numerical model. Reduction in the hydraulic properties of a deep, soft mud layer due to gradual consolidation in response to excessive pumping was examined, and the impact on the groundwater of the deep confined aquifer was determined.

Geologic and Hydrogeologic Background

Figure 1 shows the boundaries of Suzhou City and the study area. Also shown are the location of the cross section in Fig. 2 and historical structures such as the Great Canal and old city moat. The focus of the study is the area of about 180 km^2 covered by the city (Fig. 1). However, hydrologic and political boundaries do not coincide. Therefore, the actual study area is extended to 343 km^2 to include the area surrounding Suzhou City so that the impact of the uncertainties of the hydrologic boundaries on the modeling results can be minimized.

Hydrostratigraphy

The study area is covered by Quaternary deposits of fluvial, lake, lagoon and marine origins, with a total thickness of up to about 200 m. Figure 2 summarizes the hydrostratigraphy of the study area. The Quaternary sediments can be divided into 11 layers based on their geologic and hydrogeologic characteristics (Table 1). River deposits, which comprise the aquifers, are dominated by sands of various sizes. There is one unconfined aquifer and three confined aquifers. The third confined aquifer, which consists of thick and coarse river channel deposits, has the highest hydraulic conductivity and is the main aquifer of groundwater exploitation. Some interlayered lake and river deposits are rich in clay and well consolidated. They are denoted as “hard layer” in this study. There are four such layers. Most of the lagoonal and marine deposits, however, are soft to plastic, dark clay and rich in organic materials. These materials are denoted as “soft layer”. There are three soft layers in this study area, among which the third soft layer has the greatest thickness and is located near the main aquifer. Both of the soft and hard layers have poor hydraulic conductivity and can be treated as aquitard or semi-confining units.

Spatial Distributions of Hydrostratigraphic Units

There are 140 boreholes in the study area, which provide fairly detailed information on the spatial distribution of the 11 layers. Figure 3 presents thickness contour maps of the three soft layers and the three confined aquifers. It can be seen from Fig. 3A–C that clay and mud layers in the south part of the area are generally thicker than in the north part. Overall, deeper soft layers have larger thickness. The third soft layer has the greatest thickness

 DOI 10.1007/s10040-002-0225-5

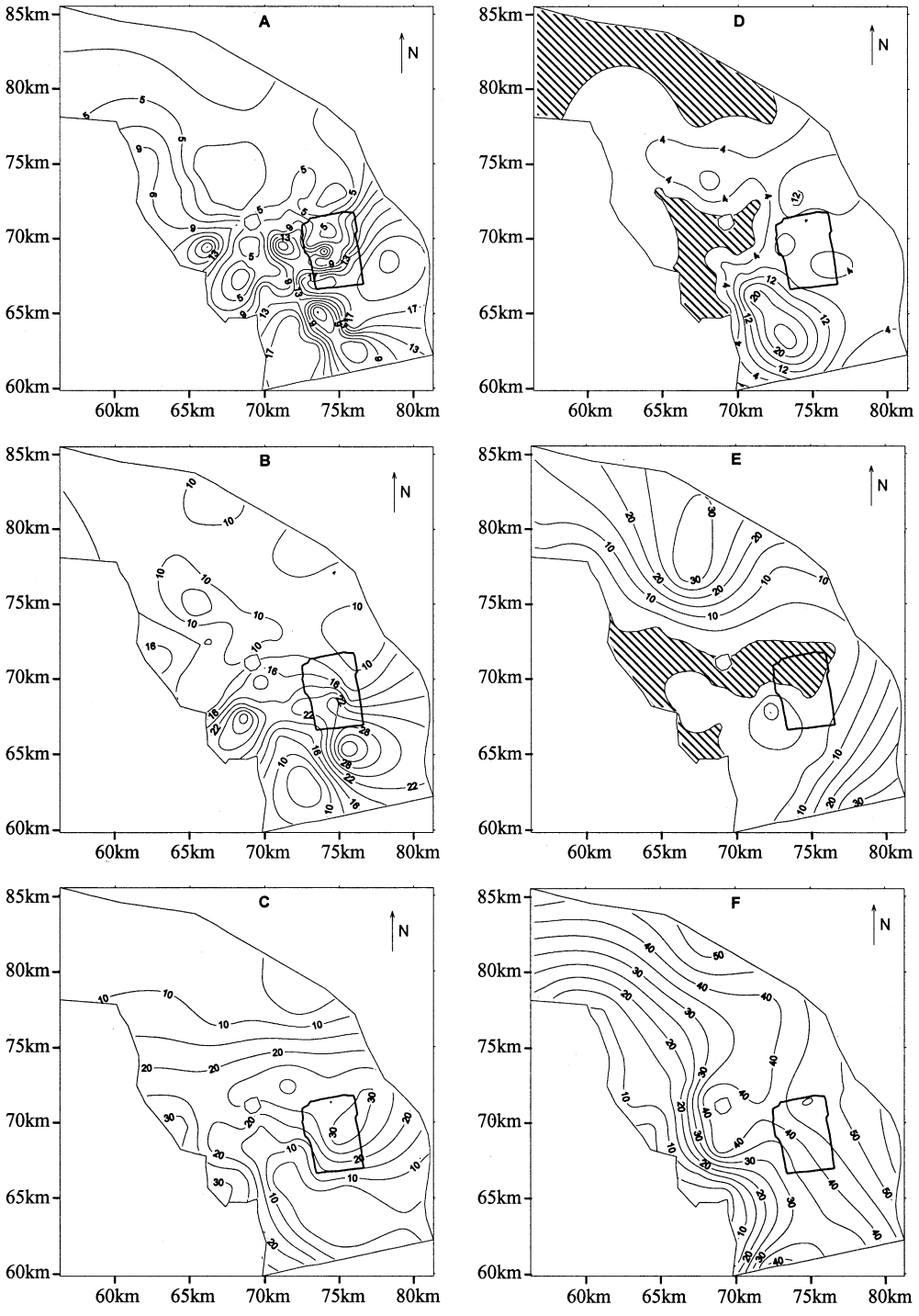

Fig. 3A–F Thickness (in m) contour maps of three soft layers (**A**–**C**) and three confined aquifers (**D**–**F**). The *square* in the center of each map is the old city moat

around the northeast corner of the city moat. Figure 3D–F shows the spatial change in thickness of the confined aquifers. The first confined aquifer is thick near the south corner of the study area and pinches out toward the north. The second confined aquifer is thick in the southeast corner and in the north but thin in the central part of the area. Overall the third confined aquifer has the greatest thickness of the three confined aquifers. Its thickness is controlled by the paleo-NW-SE river channels which occur along the northeast border of the study area. The thickness of the layer is over 30 m around the northeast part of the city moat, and on average decreases by 1 m over 100-m horizontal distance towards the southwest, as shown in Fig. 3F. More detailed spatial distributions of the hydrostratigraphic units are presented by Chen and Pei (2000). These distributions provide an important basis for aquifer parameter zonations used in the numerical modeling.

 DOI 10.1007/s10040-002-0225-5

Table 1 Hydrostratigraphy of Suzhou City area

Sequence no.	Layer type	Symbol	Deposition environment	Description	Thickness (m)
1	1st hard layer	Q_3^{2-3}	Fluvial and lake	Gray to yellow gray clay, silty clay, silt; hard	5–6
2	Unconfined aquifer	$Q_3^{2-2}-Q_3^{2-3}$	Fluvial and lake	Silty clay, silt and fine sand	4–20
3	1st soft layer	$Q_3^{2-2}-Q_3^{2-1}$	Lagoon	Gray to dark clay, interlayered clay and silt; soft to plastic	3–20
4	2nd hard layer	Q_3^{2-1}	Lagoon, lake and fluvial	Dark green clay; hard	0–16
5	1st confined aquifer	Q_3^{2-1}	Fluvial and lake	Gray to yellow silt, find sand	4–24
6	2nd soft layer	Q_3^1	Lagoon	Gray and dark gray clay and silty clay; plastic	10–20
7	3rd hard layer	Q_2^2	Fluvial and lake	Gray to dark clay with horizontal bedding, occasional sand lens; firm	0–36
8	2nd confined aquifer	Q_2^2	Fluvial and lagoon	Gray and yellow gray silt and fine sand, occasional medium sand	0–30
9	3rd soft layer	Q_2^1	Lagoon	Interlayered clay and silt, soft to very soft gray clay; soft to plastic	5–30
10	4th hard layer	Q_1^3	Fluvial and lake	Gray blue and dark yellow clay, occasional bedding; stiff	10–18
11	3rd confined aquifer	Q_1^2	Fluvial and lake	Gray coarse sand and gravel, medium to fine sand	10–50

Recharge and Discharge of the Groundwater System

Located in the subtropical monsoon zone, Suzhou City is mild and humid, with abundant rainfall in the autumn. Rain infiltration is an important source of recharge to the groundwater system. There are many surface water bodies in the study area. The major ones are Tai Lake in the west, Yangchen and Dusu lakes in the east, and the Great Canal passing from north to south through the center of the study area. These surface water bodies provide direct recharge to the shallow unconfined aquifer.

The main discharges are evaporation from the shallow unconfined aquifer and exploitation in deep aquifers. Groundwater also discharges to surface water. With the development of the economy and the increase of the population, groundwater extraction has been steadily increasing since the 1960s. Deep pumping wells have increased from eight in the 1960s to several thousands in the 1990s. In recent years, some 20 to 40×10^6 m^3 groundwater is pumped annually from the subsurface system for industrial, domestic and agriculture purposes. The third confined aquifer is the major aquifer under exploitation. Figure 4 shows a contour map of the exploitation intensity (defined as the volumetric pumping rate over a unit area) in the third confined aquifer in February 1983. Due to groundwater extraction, a large cone of depression is formed in the third confined aquifer, with the center approximately at the west of the city moat (Fig. 5). There are only a few pumping wells with limited capacity in the second confined aquifer, and there is no record of pumping in the first confined and the unconfined aquifers.

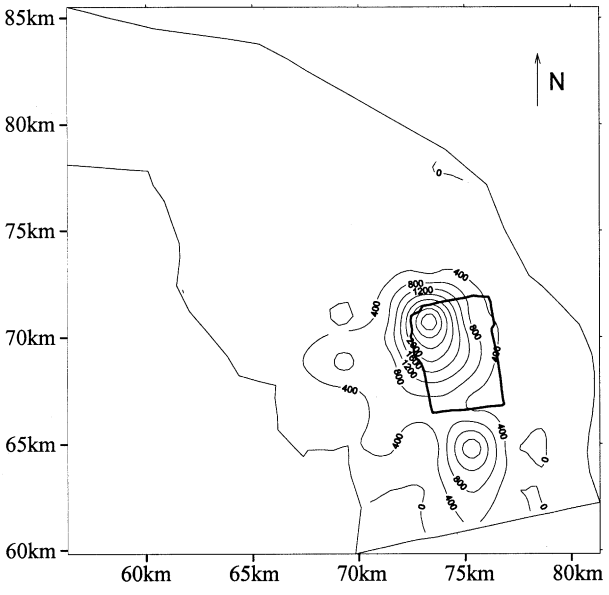

Fig. 4 Pumping intensity (m^3 day^{-1} km^{-2}) contour map for the third confined aquifer in February 1983

Monitoring Systems of Groundwater Levels and Ground Subsidence

A groundwater-level monitoring system in this area has been in operation since 1983. There are 74 monitoring wells, with 61, three, three, and seven wells in the third, second, first confined aquifers and unconfined aquifer, respectively. Most of the wells are located in the southern part of the study area (Fig. 5). The water level is measured every five days. All the extraction wells are gauged and the pumping rates have been recorded since 1984.

A ground subsidence monitoring system was introduced in 1983. About 70 ground-level marks are surveyed in every three to four years. They also are concentrated in the southern part of the area (Fig. 6). The contour map of the observed total ground settlement in

 DOI 10.1007/s10040-002-0225-5

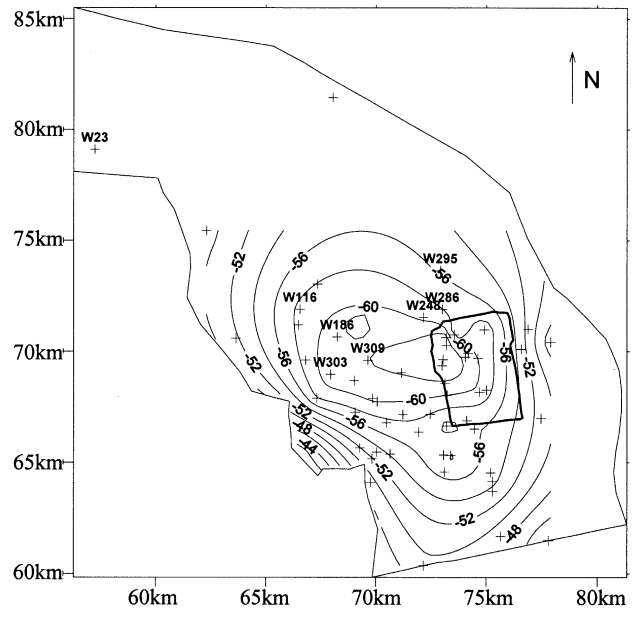

Fig. 5 Groundwater level (in m) contour map of the third confined aquifer showing a cone of depression with the center in the north part of the city moat. The *crosses* are the locations of observation wells. Wells which were randomly chosen for comparing the observed and simulated heads in Fig. 9 are annotated with *numbers*. The water level is in m

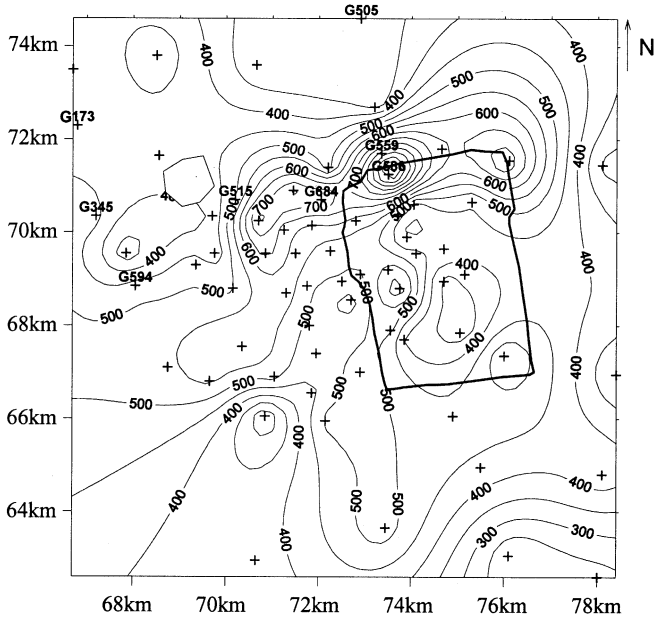

Fig. 6 Contour map of accumulated ground settlement (in mm) based on the survey in 1983–1997. The *crosses* are the locations of survey points. Only some points which are randomly chosen for comparing the observed and simulated settlement in Fig. 10 are annotated with *numbers*

1983–1997 is presented in Fig. 6. The most significant settlement occurs near the northwest corner of the city moat, with the maximum total settlement exceeding 1 m.

Numerical Presentation of the Aquifer System

Initial-Boundary Value Problem for Groundwater Flow

As discussed above, there are four aquifers and three semi-confined layers consisting of hard and soft layers. To simulate the consolidation of soft mud layers in detail, the first, second and third soft layers were further divided into three, three, and nine sublayers, respectively. The groundwater flow system in the Suzhou City area is therefore represented by 23 model layers. The initial-boundary value problem for the groundwater flow in this system can be expressed by a set of three-dimensional transient groundwater models under mixed confined and unconfined conditions (Chen and Lin 1999).

Coupling Between Groundwater Flow and Soil Consolidation

The relation between groundwater head change and soil compaction is based on the principle of effective stress developed by Terzaghi (Craig 1995), where effective stress (σ') is expressed as the difference between the total stress (σ), which is the total overburden load, and fluid or pore pressure (p):

$$\sigma' = \sigma - p \tag{1}$$

If the total overburden load is assumed to be constant, then:

$$d\sigma' = -dp$$

The definition of total hydraulic head is:

$$H = z + u/\gamma_w \tag{2}$$

So:

$$p = \gamma_w (H - z) \tag{3}$$

$$\text{or } dp = \gamma_w dH = -d\sigma' \tag{4}$$

The compressibility of the aquifer skeleton (α) is the same as the coefficient of volume compressibility m_v (Craig 1995). If water is assumed to be incompressible (the compressibility of water β=0), the specific storage becomes:

$$S_s = \gamma_w (\alpha + n\beta) = \gamma_w \alpha = \gamma_w m_v \tag{5}$$

where α is the compressibility of the aquifer skeleton, β is the compressibility of water, and n is the porosity.

The groundwater flow equation and Terzaghi's consolidation equation are linked with each other via the above relationship. The amount of consolidation S of a layer can be calculated using the storage coefficient S_s:

$$S = S_s \Delta H M$$

where M represents the thickness of the layer. If there are N layers, the total ground settlement is:

 DOI 10.1007/s10040-002-0225-5

$$S = \sum_{i=1}^{N} S_{si} \Delta H_i M_i \tag{6}$$

In the process of soil consolidation, both hydraulic conductivity K and specific storage S_s are expected to vary with the porosity. The relation between hydraulic conductivity and porosity can be derived on the basis of the following Kozeny-Carman equation (Huang 1983):

$$K \propto \frac{n^3}{(1-n)^2}$$

which further leads to

$$K = K_0 \left(\frac{n}{n_0}\right)^3 \cdot \left(\frac{(1-n_0)}{(1-n)}\right)^2 \tag{7}$$

where n_0 and n are porosity before and after consolidation, respectively, and K_0 and K are hydraulic conductivity before and after consolidation, respectively. The Kozeny-Carman equation was originally derived for sand packs. Although it does not work well for silts and clays, it is still often used to evaluate permeability from porosity in compacted shales of very low permeabilities (Ungerer et al. 1990). In this study, this relation was used approximately for both aquifers and aquitards.

The variation of specific storage S_s can be obtained from the e–log σ' curve of the consolidation experiment. The slope of such a curve is defined as the compression index C_c:

$$C_c = -\frac{de}{d(\log \sigma')} = \frac{\alpha(1+e)\sigma'}{0.434}$$

On the basis of the definition for aquifer compressibility (Fetter 2001),

$$\alpha = -\frac{dV/V}{d\sigma'} = -\frac{de}{(1+e)\,d\sigma'} = 0.434\frac{C_c}{(1+e)\sigma'} \tag{8}$$

where dV is the change in aquifer volume, V is the original volume, e is the void ratio, and $d\sigma'$ is the change in effective stress.

Considering the definition of specific storage, the following relation between S_s and void ratio e can be obtained:

$$S_s = \gamma_w \left[0.434\frac{C_c}{(1+e)\sigma'} + n\beta_w\right] \tag{9}$$

In the above formula, the compression index C_c can be used only when σ' is greater than the preconsolidation stress. Otherwise, the expansion index C_e should be used instead of C_c. Equations (7) and (9) show the K and S_s change with void ratio e (or porosity n), which in turn changes with consolidation. The consolidation in the model is treated as a nonlinear process, since key parameters are not constant.

Initial and Boundary Conditions

Boundary conditions

The west mountain boundary is chosen as a no-flow boundary. Lakes at the boundaries are set to be known-head boundaries. The Great Canal and some lakes are inside the model area and also treated as known-head boundaries. Some boundaries are not natural ones. In order to reduce the impact of uncertainties of these boundary conditions on the simulation results in Suzhou City, the model area is extended to some villages and towns far beyond Suzhou City proper (Fig. 1), so that groundwater extraction during the simulation period has no disturbance beyond these locations. These artificial boundaries are represented by fixed-head boundaries. The bottom of the Quaternary deposits is in contact with the Jurassic shale and represented by an impermeable boundary.

There are wells which intercept more than one aquifer. These wells comprise complicated internal boundary conditions due to vertical flow through the wellbore. An equivalent hydraulic conductivity (EHC) approach introduced by Chen and Jiao (1999) was employed to handle the vertical flow through the well bore. This approach uses pipe flow theory to describe the behavior of the vertical flow through the well bore, and couples this behavior with groundwater flow through aquifers and leaky confining layers. Details of this approach can be found in Chen and Jiao (1999).

Initial conditions

Considering the availability of the data, the simulation period was chosen as January 1983, when both the groundwater and ground settlement monitoring systems were in operation, to July 1997 when this research project started. The time step is one month. Altogether there are 175 time steps. The average head of the observed heads in a month is taken as the head of that month for modeling.

The initial head of each node is required before the numerical simulation is carried out. Initial heads are commonly interpolated from the observed heads in observation wells. In the study area, most of the observation wells are located in the third aquifer. There are only a few observation wells in other aquifers, and there is no observation well in the semi-confining layers. Consequently, it is impossible to obtain directly the initial heads by interpolating the observed heads.

Groundwater extraction in 1950 was minor and the groundwater at that time is assumed to be controlled mainly by rainfall and evaporation. The numerical model is run with initial hydrogeological parameters to obtain the groundwater heads in January 1950. The model was then run with the rainfall, evaporation and extraction between 1950 and 1983 to obtain the groundwater head in January 1983, which was then used as the initial head for the simulation period of January 1983 to September 1997.

Model Discretization and Parameter Zonation

The system was discretized into a series of hexahedral or wedge-shaped elements. To better depict the rapid

 DOI 10.1007/s10040-002-0225-5

Table 2 Parameter zones and estimated parameters

Soil layer	Parameter	Zone							
		1	2	3	4	5	6	7	8
		9	10	11	12	13	14	15	16
1st hard layer	K (m day^{-1})	0.01	0.01	0.001	0.001				
K_z (m day^{-1})		0.0076	0.0076	0.00076	0.00076				
	S_y	0.05	0.05	0.05	0.05				
	S_s	0.0015	0.0015	0.0015	0.0015				
Unconfine aquifer	K (m day^{-1})	0.1	1	3	6				
	K_z (m day^{-1})	0.02	0.2	0.6	1.2				
	S_y	0.1	0.12	0.15	0.2				
	S_s	0.00045	0.00009	0.000072	0.000046				
1st soft layer	K (m day^{-1})	0.001	0.001	0.001	0.001				
	K_z (m day^{-1})	0.0005	0.0005	0.0002	0.0001				
	S_s	0.0012	0.0012	0.0012	0.0012				
2nd hard layer	K (m day^{-1})	0.02							
	K_z (m day^{-1})	0.0078							
	S_s	0.00081							
1st confined aquifer	K (m day^{-1})	0.02	1	3	6	7			
	K_z (m day^{-1})	0.008	0.05	0.6	1.2	1.4			
	S_s	0.000028	0.000028	0.000028	0.000028	0.000028			
2nd soft layer	K (m day^{-1})	0.003	0.001	0.003					
	K_z (m day^{-1})	0.0003	0.0003	0.0003	0.0006				
	S_s	0.0012	0.0012	0.0012	0.0012				
3rd hard layer	K (m day^{-1})	0.02							
	K_z (m day^{-1})	0.0052							
	S_s	0.00048							
2nd confined aquifer	K (m day^{-1})	10	13	17	17	25			
	K_z (m day^{-1})	2	2.6	3.4	3.4	5			
	S_s	0.00003	0.00003	0.00003	0.00003	0.00003			
3rd soft layer	K (m day^{-1})	0.001							
	K_z (m day^{-1})	0.000585							
	S_s	0.0012							
4th hard layer	K (m day^{-1})	0.002							
	K_z (m day^{-1})	0.00008	0.000204	0.000204	0.000055	0.000138	0.000533	0.00022	0.00104
		0.000057	0.000050	0.000151	0.00199	0.00017	0.0004	0.0015	
	S_s	0.0003	0.0003	0.0003	0.0003	0.0003	0.0003	0.0003	0.0003
		0.0003	0.0001	0.0006	0.0002				
3rd confined aquifer	K (m day^{-1})	17.6	28.4	34.4	10.4	13.52	8.92	20.6	33.2
		8.96	10.34	8.3	14.2	26.4	33.4		
	K_z (m day^{-1})	3.2	5.28	6.3	2.01	2.07	1.8	4.1	6.6
		1.8	2.07	1.7	2.8	5.3	6.7		
	S_s	0.00001	0.000006	0.000009	0.00001	0.00001	0.00001	0.00001	0.000006
		0.00001	0.00001	0.00001	0.000006	0.000006	0.000004		

change of water levels near major pumping wells, the elements are progressively finer toward these wells. Details of the mesh system in plan are shown in Fig. 7. Each layer is represented by 936 nodes and 1,775 elements. The entire model of 23 layers has 21,528 nodes and 40,825 elements. A finite difference method with random polygon grids (Chen and Tang 1994) is used to solve the numerical groundwater flow model.

Many aquifer parameters are involved, owing to the complexity of the aquifer system. These parameters include horizontal and vertical hydraulic conductivities, storativities, specific yield, etc. For each layer, the area is divided into different parameter zones (Table 2). Altogether there are 183 parameters. The zonation of the four aquifers is presented in Fig. 8. The third confined aquifer, which is the most important aquifer, is divided into 14 zones. Other less important aquifers are divided into only four to five zones. These zones are entirely based on the topographical location, geology, and soil and rock types (Chen and Pei 2000). The zonation has not been calibrated but the parameters of each zone were calibrated in the numerical model. An initial assessment and its possible range for each of the parameters are obtained based on the various geologic and hydrogeologic reports, pumping test data and other literature from previous studies. Both the trial-and-error method and the Fibonacci optimization method (Chen and Tang 1994) were used to calibrate the model against observed data, to achieve the smallest possible objection function which is defined as the sum of the squares of the differences between the observed and calculated results, including both water level and ground settlement.

 DOI 10.1007/s10040-002-0225-5

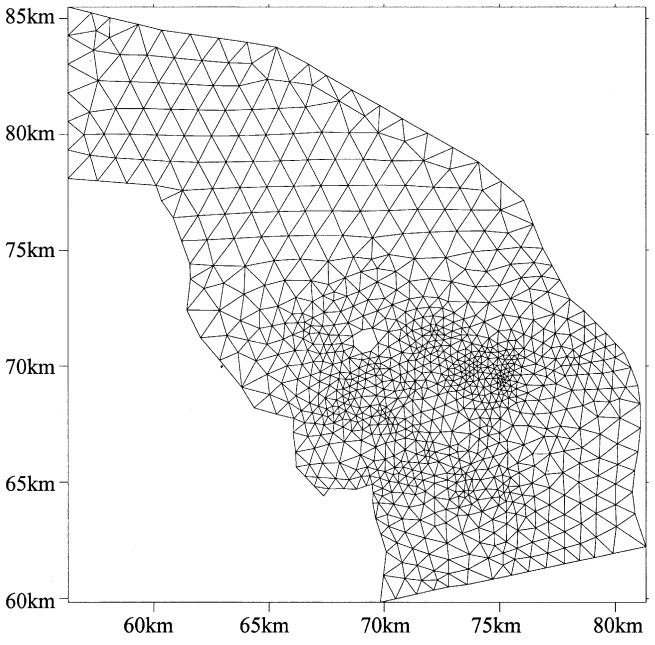

Fig. 7 Plan view of model discretization

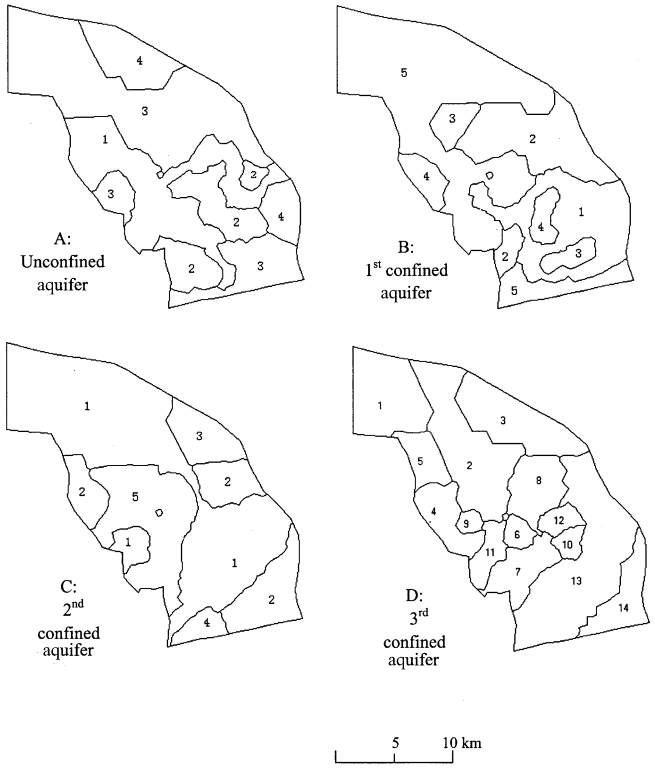

Fig. 8A–D Parameter zonation of four aquifers on the basis of geology

Modelling Results and Discussion

After calibration, the average infiltration rate (defined as the ratio of infiltrated water to the water table and rainfall) is estimated to be 30%, and the compression index is estimated to be 0.2. Other estimated parameters change with parameter zones and are shown in Table 2. Nonuniqueness is inevitable, considering the large number of parameters, but the estimated parameter values agree closely with the lateral and vertical distributions of the geologic materials.

Table 3 Statistics of the relative errors in simulated heads

Aquifer	Relative error (%)					
	<5	5–10	10–20	20–30	30–50	>50
3rd confined	37.86	23.59	15.84	3.03	0.76	0
2nd confined	1.07	1.02	1.09	0.74	0.54	1.42
1st confined	0.07	0.24	0.29	0.42	0.07	4.10
Unconfined	0.98	0.78	1.47	1.14	1.56	1.91

Comparisons of the Simulated and Observed Results

Eight monitoring wells were randomly chosen among the total 61 monitoring wells in the third confined aquifer for comparison of observed and simulated heads (Fig. 9). Overall the match between the observed and simulated heads is acceptable. Although not showed here, the contour maps of simulated water levels were constructed and compared with the observed groundwater contour maps. It is believed that the overall features of the spatial water-level distribution in the third confined aquifer, such as the maximum drawdown and its location, are well reproduced by the numerical model. The fit between the simulated and observed heads in the unconfined aquifer is also reasonable. The fit for the first confined aquifer is, however, relatively poor.

To provide information on the overall match of all the monitoring wells, including those in the unconfined, first, and second confined aquifers, Table 3 presents some statistics concerning the relative error in the simulated water levels. The relative error is defined as the absolute difference between the simulated water level and the observed water level divided by the observed water level. For the third confined aquifer, there is no simulated water level with relative error >50%, and over 60% of the water levels have relative errors <10%. The fit in the other aquifers is not as good. Especially for the first confined aquifer, over 4% of the simulated water levels have relative error >50%. The poor match in other aquifers may be caused by several factors, including (1) the monitoring wells are too few to adequately define the initial head distributions in these aquifers; (2) the two aquifers are not the main aquifers under exploitation; and (3) the complicated aquifers structures are probably not well revealed by the monitoring system. It is suspected that some wells in the unconfined aquifer may be dug by village people, but they are not included in the model due to lack of record.

Similarly, eight consolidation survey points out of 32 survey points were randomly chosen for comparison be-

 DOI 10.1007/s10040-002-0225-5

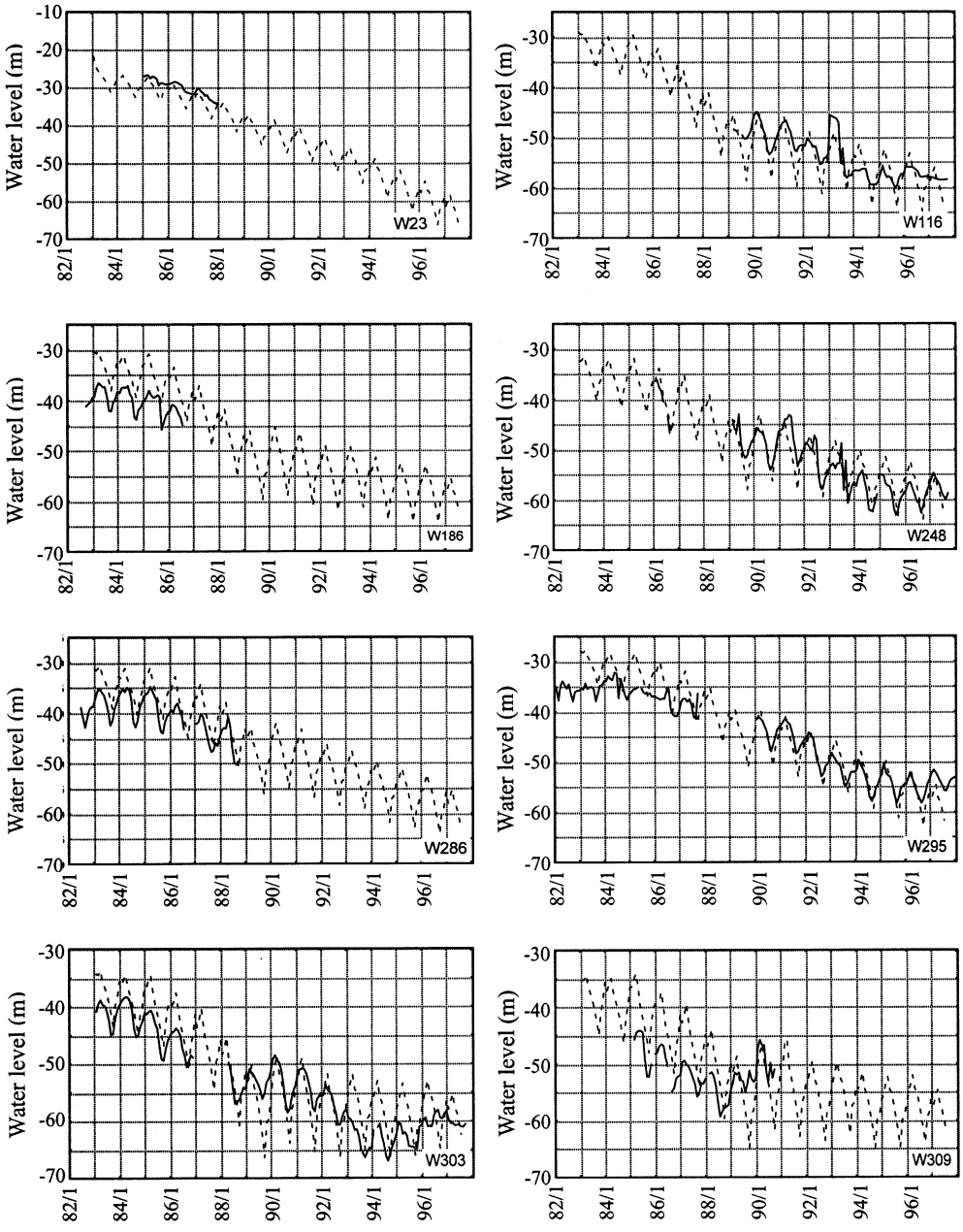

Fig. 9 Comparison between observed (*solid lines*) and simulated (*dotted lines*) water levels in eight randomly chosen observation wells (dates given as year/month)

Table 4 Statistics of the relative errors in simulated settlement

	Relative error (%)			
	<5	5–10	10–20	>20
Percentage	45.7	24.3	15.7	14.3

tween simulated and observed subsidence. The fit was fairly good. Figure 10 shows the observed and simulated ground subsidence at the eight survey points. Similar statistics concerning the relative errors were also calculated and are shown in Table 4. It can be seen that about 46% of the survey points have a simulated settlement error of <5%. The contour map of the simulated accumulated ground settlement was constructed (not shown here) and compared with the observed ground settlement contour map. The simulated maximum ground settlement and its location are close to the observed results, although the simulated map shows a more complicated pattern.

Change of Water Level, Porosity and Hydraulic Conductivity with Time

The numerical model can simulate the change of porosity and hydraulic conductivity with the process of consolidation. Figure 11 presents the change of the two parameters with time at the middle of the third soft layer around the center of the settlement. It can be seen that

 DOI 10.1007/s10040-002-0225-5

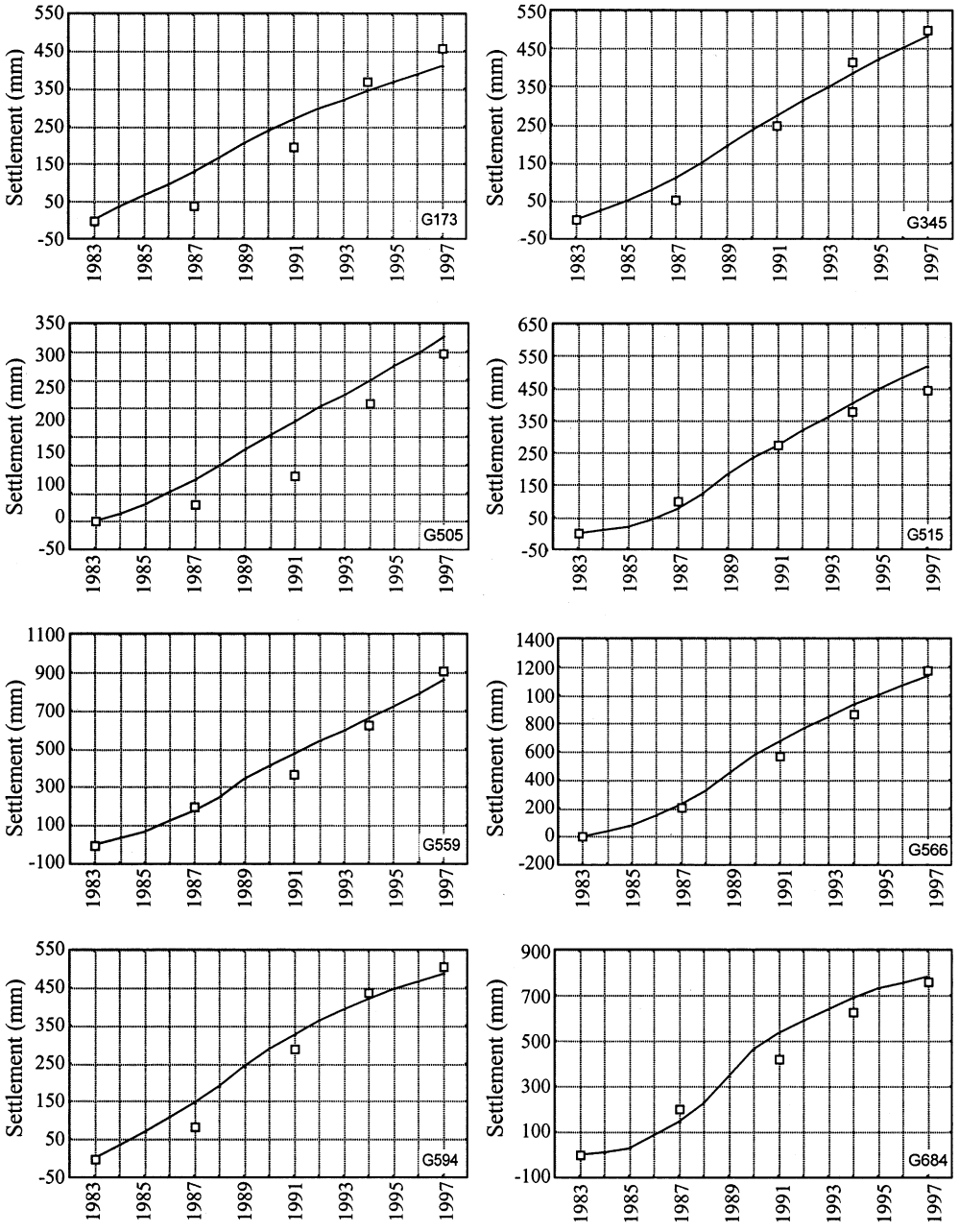

Fig. 10 Comparison between observed (*squares*) and simulated (*solid lines*) ground settlement in eight randomly chosen survey points (dates given as year)

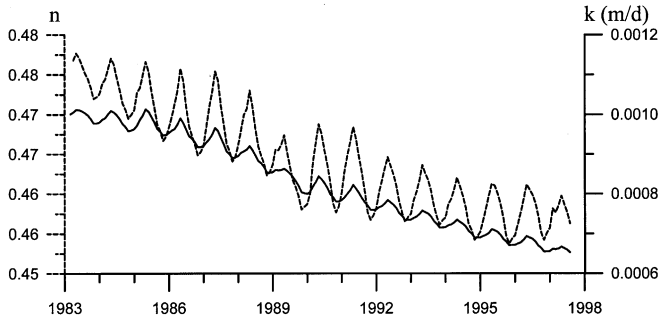

Fig. 11 Temporal changes of porosity (*broken line*) and hydraulic conductivity (*continuous line*) at the middle of the third soft layer around the center of the ground settlement

the porosity changes from 0.477 in 1983 to 0.442 in 1997. The reduction is over 7%. In the same period, the hydraulic conductivity is reduced from 0.00101 to 0.00067 m day^{-1}. The reduction is almost 34%. The hydraulic properties are expected to be modified further should the overexploitation continue.

The reduction in the hydraulic conductivity of the third soft layer may have significant impact on the groundwater resource of the deep, confined aquifer. For such a deep aquifer, the recharge from the overlying, shallow aquifers through the semi-confining layer is the only source. Since the hydraulic conductivity of the soft layer is reduced, the recharge to the underlying aquifer is expected to reduce accordingly. It is believed that the decline in water level of the confined aquifer is caused not

 DOI 10.1007/s10040-002-0225-5

only by the continuous pumping but also by the reduction in the recharge through the mud layer.

It is believed the general conclusions of the above discussion on the reduction of hydraulic conductivity of the soft layers with time is correct, but it should be pointed out that the estimated amount of hydraulic conductivity reduction may be quite uncertain, since the Kozeny-Carman relation used here was originally derived for sand packs.

Importance of Spatial Distribution of Soft Layer on Ground Settlement

It is interesting to note that the center of the ground settlement (Fig. 6) and that of the cone of depression (Fig. 5) do not coincide. The maximum settlement is located in the north part of the city moat whereas the maximum drawdown is located in the west part of the moat. This is because the ground settlement is controlled not only by the drawdown but also by the thickness of the clay layers, as can be seen from Eq. (6). The ground settlement in this area is mainly contributed by consolidation of the third soft layer. It reaches its maximum thickness near the northeast corner of the city moat, as can be seen from Fig. 3C. The ground settlement is the superposition of the effects of the drawdown of water level and the thickness of the soft layer. That is probably why the maximum ground settlement is located at the north border of the city moat (Fig. 6), which is somewhere between the area of the maximum drawdown and the area of maximum thickness of the soft mud.

Since the total subsidence is controlled by drawdown, thickness, and the coefficient of volume compressibility of all the layers, the spatial distribution and maximum of the ground settlement would be different if the distribution of the pumping wells were designed by considering the distribution of the soft layers. It seems possible that less severe ground subsidence would be obtained if fewer pumping wells were installed in areas with thick, soft layers. The numerical model can be used to study this hypothesis.

Under the current pumping conditions, the total accumulated ground settlement in the center of the subsidence contour is 1,187 mm. The compression of the third soft layer is 994 mm, which is 84% of the total settlement. Although groundwater conditions in all the layers and the consolidation in all the soft layers will have impact on the total ground settlement, the discussion below will focus on the third soft layer, since the consolidation of this layer contributes most to the ground settlement due to its large thickness and short distance to the main pumped aquifer.

With the total water pumped being kept fixed, the pumping rates of the wells are now readjusted so that their rates are roughly inversely proportional to the thickness of the third soft layer, that is, an area of large thickness of mud is given a small pumping rate. The numerical model can be run again under such a hypothetical pumping condition. The total maximum settlement will be now only 901 mm. Compared to the original 1,187 mm, the total settlement would be reduced by over 24%. It can be seen that the distribution of extraction wells is important in controlling the ground settlement. The above recalculation is a simple calculation considering only the third soft layer. If a rigorous optimization model is used by considering the thickness and the coefficient of volume compressibility of other soft layers, the thickness of the hard layers and aquifers, and the boundary conditions, a more optimal pumping rate distribution can be achieved and the ground settlement may be further reduced.

Conclusions

The geology and hydrogeology in the Suzhou City area were investigated to understand the hydrostratigraphy of the aquifer system. The aquifer system is conceptualized into four aquifers and seven semi-confined layers. The third confined aquifer, which is the main aquifer under pumping, and the third soft layer, which has the largest thickness and is closest to the main aquifer of all the soft layers, are the focus of the study. An examination of historical data of groundwater level and ground settlement indicates that there is a close relation between the ground subsidence and groundwater exploitation. A three-dimensional numerical model which couples the groundwater flow and soil consolidation was developed to investigate the mechanisms of ground settlement. By calibrating the model with both groundwater-level and ground-settlement measurement data, the aquifer parameters of the system were estimated. The model outputs fit reasonably well with the observed results, which indicates that the numerical model can reproduce the dynamic processes of both groundwater flow and soil consolidation over the simulation period. The study also shows that the spatial distribution of soft clay layers is a key factor in controlling the overall ground settlement. A simple modification in pumping rates on the basis of the spatial distribution of the thick soft layer could significantly reduce the ground settlement. The hydraulic conductivity of the deep soft layer near the center of the ground settlement has been reduced by over 30% in the last 14 years. The reduction of the recharge to the deep, confined aquifer due to the decrease in the hydraulic conductivity of the soft layer may speed up the decline in the water level of the confined aquifer. The excessive groundwater extraction may not only cause ground settlement but also have adverse effect on sustainable water resources of the deep aquifer.

Acknowledgements The authors are very grateful for the careful and constructive comments by John Bredehoeft and an anonymous referee.

 DOI 10.1007/s10040-002-0225-5

References

Abidin HZ, Djaja R, Darmawan D, Hadi S, Akbar A, Rajiyowiryono H, Sudibyo Y, Meilano I, Kasuma MA, Kahar J, Subarya C (2001) Land subsidence of Jakarta (Indonesia) and its geodetic monitoring system. Nat Hazards 23(2–3):365–387

Bell FG, Cripps JC, Culshaw MG (1986) A review of the engineering behaviour of soils and rocks with respect to groundwater. In: Groundwater in engineering geology. Geol Soc Eng Geol Spec Publ 3:1–23

Chen CX, Jiao JJ (1999) Numerical simulation of pumping tests in multilayer wells with non-Darcian flow in the wellbore. Ground Water 37(3):465–474

Chen CX, Lin M (1999) Groundwater hydraulics (in Chinese). China University of Geosciences Publishing House, Wuhan

Chen CX, Pei SP (2000) Numerical simulation on ground subsidence due to ground water exploitation in Suzhou City and investigation on measures of controlling the subsidence (in Chinese). Institute of Environmental Geology, China University of Geosciences, Wuhan

Chen CX, Tang ZH (1994) Numerical methods of groundwater flow problem (in Chinese). China University of Geosciences Publishing House, Wuhan

Craig RF (1995) Soil mechanics, 5th edn. Chapman & Hall, London

Fetter CW (2001) Applied hydrogeology, 4th edn. Prentice Hall, London

Huang WX (1983) Engineering properties of soil (in Chinese). Water and Electricity Publishing House, Beijing

Lewis RW, Schrefler B (1978) Fully coupled consolidation model of subsidence of Venice. Water Resources Res 14(2):223–230

Poland JF, Davis GH (1969) Land subsidence due to withdrawal of fluids. In: Varnes DJ, Kiersch G (eds) Reviews in Engineering Geology, vol 2. Geol Soc Am, Boulder, pp 187–269

Pratt WE, Johnson DW (1926) Local subsidence of the Goose Creek oil field. J Geol 34:577–590

Ungerer P, Burrus J, Doligez B, Chenet PY, Bessis F (1990) Basin evaluation by integrated two-dimensional modeling of heat transfer, fluid flow, hydrocarbon generation, and migration. AAPG Bull 74:309–335

 DOI 10.1007/s10040-002-0225-5